CHAPTER 100

MATHEMATICAL MODELING OF LARGE OBJECTS IN SHALLOW WATER WAVES AND UNIFORM CURRENT

by

Hsiang Wang

University of Delaware, Newark, Delaware

Abstract

A mathematical model is presented which portrays the physical system of a large axially symmetric structure in a flow field of finite water depth, large amplitude wave and strong current. The flow field, which enters as the input, is derived from a velocity potential similar to that of the cnoidal wave of Keulegan and Patterson. The inclusion of a uniform velocity in the derivation of velocity potential results in a cross interference term in addition to the well known Doppler shift effect.

The numerical results are compared with experiments on a bridge pier (Ref. 6) which is partially cylindrical with base diameter equivalent to 100 feet in prototype; close to the surface, where the wave action is greatest it is conical. These results are also compared with theoretical calculations based on linear wave theory and fifth-order wave theory. It is concluded that the results based on the modified cnoidal wave theory come closest to the experimental value.

Introduction

A computer simulation is developed which portrays the physical system of an arbitrarily shaped large structure situated in a flow field where the water depth is finite, the wave is large and the current is not negligible. The structure is large in the sense that its charcteristic length is at least the same order of magnitude as wave length; the wave is large and the water is shallow in that the ratio of wave height to water depth is not infinitesimal. While the presence of a large structure causes wave reflection and diffraction, the existence of a uni-directional current results in the modification of the wave kinematics and, possibly, causes wake formation. As a consequence of large amplitude waves, the convective inertia cannot be neglected. The combination of a large amplitude wave and a large object makes it necessary to compute the wet line around the structure.

The present study is motivated by an earlier experimental work (Wang, 1970). Those laboratory measurements were performed to determine pressures, forces and moments exerted on a large bridge pier. This bridge pier had a cylindrical base and a conical top. When converted from a model into a prototype, such a bridge pier, with a base diameter of 100 feet, would be situated in water 100 feet deep with waves up to 25 feet and current up to 8 knots. The experimental results were later compared with theoretical calculations based on linear wave theory (MacCamy and Fuch, 1954) and on fifth-order wave theory (Clavier, 1967). The comparisons were unfavorable as both theories yielded much too small maximum horizontal forces and moments compared to the experimental values. Since physical situations similar to those described are quite common in engineering, a better predictive technique is, therefore, attempted.

The incoming wave field, in the absence of objects, is first derived from the cnoidal wave of Keulegan and Patterson (1940) incorporated with the effect of a uniform current. The incorporation of a current is not a trivial task as non-linear interaction occurs which results in dispersions of both wave amplitude and wave length.

Since the obstacle is not necessarily in cylindrical shape, the outflows created by the obstacle cannot be expressed in terms of known functions such as Bessel functions of the second kind used by MacCamy and Fuch. A near field wave is sought through Taylor's expansion of wave potential at the obstacle. The outflow potential at the obstacle is then expressed in terms of inflow wave potential and its derivatives normal to the object. The normal derivatives are introduced to fulfill the non-linear free surface condition. Physically, one can reason that the scattering of an incoming wave at a distance should be proportional to the variations of the incoming wave from the distance to the object.

Because of the complicated nature of the problem a computer program is developed using the Burroughs 5500 to facilitate numerical computations of pressure distributions, forces, and moments exerted on the structure.

Incoming Flow

In this section we shall seek a solution for surface waves of finite height superimposed on a uniform current in water of finite depth in the absence of the obstacle. Flow characteristics derived from the wave field will be used as the incoming flow conditions.

General Equations

It will be supposed that the velocity field is irrotational and the fluid is incompressible:

$$\vec{u}' = -\nabla\phi' \tag{1}$$

and

$$\nabla^2\phi' = 0 \tag{2}$$

where $\vec{u}'$ is the velocity vector and ϕ' is the corresponding velocity potential.

A solution of ϕ' will be sought that satisfies the appropriate boundary conditions. Referring to Fig. 1 where the uniform velocity U is oriented into the positive x-direction, we can separate the velocity potential ϕ' into two parts:

$$-\phi' = Ux - \phi \tag{3}$$

where ϕ is the unsteady part of the velocity potential. Then, we have

$$-\phi'_x = U - \phi_x = U + u \tag{4}$$

and

$$-\phi'_y = -\phi_y = v \tag{5}$$

where the subscripts refer to derivatives (as will be used throughout this paper) and where u and v are time-periodic velocities in the x and y directions, respectively.

The boundary conditions to be satisfied are at the surface, i.e., $y = \eta + h$

$$\frac{p}{\rho} = -g(y - h) + \phi_t + U\phi_x - \frac{1}{2}(\phi_x^2 + \phi_y^2) = 0 \tag{6}$$

and

$$\frac{d}{dt}[y - (\eta + d)] = 0 \tag{7}$$

where η is the free surface variation with respect to the calm water and

$$\frac{d}{dt} = \frac{\partial}{\partial t} + \nabla\phi\cdot\nabla \tag{8}$$

and at the bottom, $y = 0$

$$\phi_y = 0 \tag{9}$$

For shallow water waves, we adopt for the potential ϕ the power series (Keulegan and Patterson, 1955):

$$\phi = \sum_{n=0}^{\infty} \phi_n y^n, \quad \phi_1 = 0 \tag{10}$$

Substituting this expression for ϕ in Eq. (2), the following series is obtained

$$\phi = \phi_o - \frac{y^2}{2!}\frac{\partial^2\phi_o}{\partial x^2} + \frac{y^4}{4!}\frac{\partial^4\phi_o}{x^4} - \frac{y^6}{6!}\frac{\partial^6\phi_o}{\partial x^6} + \ldots \tag{11}$$

Differentiating with respect to y,

$$\frac{\partial\phi}{\partial y} = -y\frac{\partial^2\phi}{\partial x^2} + \frac{y^3}{3!}\frac{\partial^4\phi_o}{\partial x^4} - \frac{y^5}{5!}\frac{\partial^6\phi_o}{\partial x^6} + \ldots \tag{12}$$

The function ϕ_o is a function of x and t only.

First Order Solutions

If the velocity square terms in Eq. (6) are negligible in comparison with gh and the expansions in Eqs. (11) and (12) are cut short at the first term, wave equations of the first order can be derived. Since (in our case) we are not particularly interested in infinitesimal waves detailed presentations of first order appromimation are omitted. It is sufficient to point out that, to the first order, the effect of a uniform stream superimposed on a wave field is the well-known Doppler shift, i.e.,

$$C_1 = U + C_o = U \pm \sqrt{gh} \tag{13}$$

and

$$\omega_1 = \sigma + kU \tag{14}$$

where C is the apparent wave celerity with current
C_o is the wave celerity with no current and is equal to $\sqrt{gh}$ for the shallow water cause
ω_1 is the apparent wave frequency with current
σ is the wave frequency with no current
k is the wave number which remains unchanged with and without the current.

Second Order Solutions

When the ratio of wave height to water depth becomes appreciable, such as the present situation, first order approximation is no longer satisfactory. Second order approximation is sought, therefore. Retaining two terms in Eqs. (11) and (12) and substituting them into Eqs. (2), (6), and (7), the following set of equations are obtained:

$$(g + \frac{UC_o}{h})\eta - \frac{\partial\phi_o}{\partial t} + \frac{g}{2}\left[\frac{\eta^2}{h} + h^2(1 + \frac{U}{C_o})\frac{\partial^2\eta}{\partial t^2}\right] = 0 \tag{15}$$

and

$$\frac{\partial \eta}{\partial t} - h \frac{\partial^2 \phi_o}{\partial x^2} + U \frac{\partial \eta}{\partial x} + C_o \frac{\partial}{\partial x} \left(\frac{\eta^2}{h} - \frac{h^2}{6} \frac{\partial^2 \eta}{\partial x^2} \right) = 0 \tag{16}$$

Eliminating ϕ_o from the above equations results in the following expressions for the water surface variation (η):

$$\eta_{tt} = (C_o + U)^2 \eta_{xx} + gh\left[\left(\frac{3}{2} + \frac{U}{C_o} \right) \frac{\eta^2}{h} + \frac{h^2}{3} \left(1 + \frac{U}{C_o} \right) \frac{\partial^2 \eta}{\partial x^2} \right] \tag{17}$$

This equation is valid to the second order approximation. The corresponding wave celerity can be shown as equal to:

$$C_2 = U + C_o \left[1 + \frac{1}{4} \frac{(3 + 2U/C_o)}{1 + U/C_o} \frac{h}{\eta} + \frac{1}{6} \frac{h^2}{\eta} \eta_{xx} \right] \tag{18}$$

In the absence of a current the above expression reduces to

$$C_2' = C_o \left(1 + \frac{3}{4} \frac{\eta}{h} + \frac{1}{6} \frac{h^2}{\eta} \eta_{xx} \right) \tag{19}$$

which is the same as that obtained by Keulegan and Patterson (1940). Thus, to the second order, simple Doppler's shift is not applicable. An interference term:

$$\frac{1}{4} \frac{(3 + 2U/C_o)}{1 + U/C_o} \frac{\eta}{h} \tag{20}$$

exists. This term manifests the fact that the uniform current not only transports the waves but also does additional work on them. Longuet-Higgins and Stewart (1960) have found a similar term for deep water waves and have defined a radiation stress tensor to express the work done by a current of unit strength against the waves. This interference term can be rewritten as

$$\gamma(U/C_o) \cdot \frac{\eta}{h} \tag{21}$$

where (U/C_o) is a function of U/C_o alone. When this function is plotted against U/C_o as shown in Fig. 2, the effects of current on waves is clearly illustrated. For the condition of counter current, that is U/C_o is negative, energy is fed into the wave; the wave steepens and finally breaks. For the condition of concurrent, on the contrary, energy is extracted from the wave and the wave flattens. All of these phenomena are commonly observed but cannot be explained so far without an energy exchange mechanism.

The water surface variation can also be expressed explicitly by solving Eq. (15) with the assumption of a permanent wave form, i.e.,

$$\frac{d\eta}{dt} = \frac{\partial \eta}{\partial t} + C_2 \frac{\partial \eta}{\partial x} = 0 \tag{22}$$

or

$$\frac{\partial \eta}{\partial t} = - C_2 \frac{\partial \eta}{\partial x} \tag{23}$$

Following closely the derivations outlined by Keulegan and Patterson (1940) by substituting Eq. (20) into Eq. (15) and integrate twice one obtains

$$\eta = - \eta_2 + H\, Cn^2\left[\sqrt{\frac{3C + 2U}{4(C+U)h^3}}\ \frac{1}{k}\ \sqrt{H}\,(x - C_2 t), k\right] \tag{24}$$

where H is the wave height
Cn is one kind of the Jacobian functions of modulus k which is related to wave length (see Eq. (23)), and

$$\eta_2 = H\left[\frac{E_1(k) + k^2 - 1}{F_1(k)k^2}\right] \tag{25}$$

$F_1(k)$ and $E_1(k)$ are the elliptic integrals of the first and second kind respectively. The wave length is found to be

$$L = \sqrt{\frac{16(C_o + U)h^3}{(3C_o + 2U)H}}\ kF_1(k) \tag{26}$$

which is seen to be a function of the uniform velocity. Differentiating Eq. (21) twice and then substituting into Eq. (16), one obtains the speed of the wave crest as:

$$C_{c2} = U + C_o\left[1 + \frac{3 + 2U/C_o}{8\ (1 + U/C_o)}\frac{H}{h} + \frac{16}{3} F_1{}^2(k)\ \frac{h^2}{L^2}\right] \tag{27}$$

If we define T as the wave period, we have by definition

$$C_{c2} T = L \tag{28}$$

From Eqs. (23), (24) and (25), the effects of current on wave length as well as on wave height can be brought out. Referring to Fig. 3, it becomes obvious that for the case of counter current the wave length shortens, whereas the reverse is true for the case of concurrent flow. Figure 4 shows the effects of current on wave height. As expected, for counter current, the wave height increases whereas for concurrent flow the wave height diminishes.

The velocity potential of the incoming flow field can be obtained from Eq. (16). We first substitute η_t by $-\frac{\partial(\eta C_2)}{\partial x}$ into Eq. (16) and then integrate it with respect to x twice

$$\phi_o = \frac{1}{h}\int (U - C_2)\eta dx + \frac{g}{2h^2}\int \eta^2 dx - \frac{gh}{12}\eta_x \tag{29}$$

The task now reduces to an evaluation of $\int \eta dx$ and $\int \eta^2 dx$. The integrations are lengthy but straightforward. The resulting ϕ_o becomes:

$$\phi_o = a + b + c \tag{30}$$

where

$$a = \frac{U - C_2}{h} \left\{ \frac{HLE(\phi)\ (k)}{2F_1(k)k} + z_d x + \frac{HL(1 - k)}{k}\ \theta \right\}$$

$$b = \frac{g}{2h^2} \left\{ z_d^2 x + 2 z_d a + H^2 \left[\frac{1}{3}\ \mathrm{snX\ cnX\ dnX} + \frac{2 + k^2}{3k^4} F_1(\phi)\ (k) - \frac{2(1 + k^2)}{3k^4}\ E_1(\phi)\ (k) \right] \right\}$$

$$c = - \frac{gh}{12} \times 4\ \frac{H}{L} F_1(k)\ \mathrm{snX\ cnX\ dnX}$$

$$= - \frac{1}{3}\ gh\ \frac{H}{L} F_1(k)\ \mathrm{snX\ cnX\ dnX}$$

where

$$\phi = \sin^{-1} [\mathrm{snX}]$$

and

$$X = \left[2F(k)\ \left(\frac{x}{L} - \frac{t}{T} \right),\ k \right]$$

Outflow Generated by the Obstacle

Since the characteristic length of the obstacle is, in the present suudy, assumed to be comparable to that characteristic of the wave field, the disturbance to the flow field created by the obstacle must be taken into consideration. In other words the outflow generated by the obstacle must be determined. Because an exact irrotational solution for a pile of irregular shape in a gravity wave field has not been found, an approximate solution is proposed to yeild near field flow information from which pressure and force on the pile can be calculated.

As the surface of the obstacle is bounded by closed curves, it is natural to define its contour in appropriate cylindrical coordinates (R, θ, y) (Fig. 5):

$$R = R\ (\theta, y) \tag{31}$$

where R prescribes the contour of the obstacle. A local coordinate system (ℓ, m, n) is also defined such that ℓ is tangent to the contour curve, m is the bi-normal, and n is the normal at any station.

The near field potential is expressed in Taylor's series of velocity potential on the obstacle:

$$\phi = \sum_{k=0}^{\infty} \frac{n^k}{k!} \frac{\partial^k \phi(p)}{\partial n^k} \tag{32}$$

where $\phi(p)$ is the velocity potential at the obstacle and n is the local normal as defined earlier.

The task now reduces to finding the velocity potential on the object.

The velocity potential on the object can be separated into two parts:

$$\phi(p) = \phi_{in}(p) + \phi_{out}(p) \tag{33}$$

where $\phi_{in}(p)$ is the inflow velocity potential that exists if the object is removed and $\phi_{out}(p)$ is the velocity potential generated by the obstacle.

The inflow velocity potential on the object is determinable from the inflow potential described in the previous section. The outflow potential on the object needs to be developed. We assume that $\phi_{out}(p)$ can be expanded in terms of functions determinable from $\phi_{in}(p)$ and its derivatives in the normal direction, i.e.,

$$\phi_{out}(p) = \sum_{k=0}^{\infty} \alpha_k \frac{\partial^k \phi(p)}{\partial n^k} \tag{34}$$

This assumption is believed to be valid for several reasons. From the point of view of mechanics, the response must be determinable from the excitation. From the mathematical point of view, many exact solutions exist in which the outflow potential created by the obstacle is, on the surface of the obstacle, proportional to the incoming potential. Outstanding examples are a submerged cylinder and a sphere. For a submerged cylinder, for instance, the outflow potential at the surface of the cylinder is equal in magnitude, to the inflow potential at the surface. Furthermore, the non-linearity of the free surface is none other than the continuous scatterings of the incoming flow by the obstacle at a distance. Thus, it is plausible to include normal derivative terms of incoming flow potential in the representation of outflow potential.(i.e., ϕ_{out} depends on the variations of ϕ_{in} with distance to the obstacle).

After one has selected the functional representations of outflow potential, the coefficients, α, can be determined through appropriate boundary conditions. These boundary conditions are:

$$p \approx 0 \tag{35}$$

$$\frac{dp}{dt} = \frac{\partial p}{\partial t} + \nabla\phi \cdot \nabla p = 0 \tag{36}$$

at the free surface. And

$$\frac{\partial \phi}{\partial n} = 0 \tag{37}$$

at the surface of the obstacle and at the bottom. These equations, (35), (36) and (37), are applied to the total potential, of course.

Since we are interested in the velocity potential at the obstacle, simultaneous solution of Eqs. (35) and (36) defines a wet line on the obstacle. It should be noted that for a finite term of expansion of ϕ_{out}, the conditions p = 0 and dp/dt = 0 cannot be satisfied exactly. One usually has to settle for an approximation such as

$$|p|_{max} \leq \Gamma_1$$

or

$$\left|\frac{dp}{dt}\right|_{max} \leq \Gamma_2$$

where Γ_1 and Γ_2 are the pre-determined maximum tolerable errors.

Once we determine the velocity potential, the pressure distribution around the obstacle can be obtained through Bernolli Equation. The total force and moment exerted on the obstacle are then calculated through numerically integrating the following equations:

$$F = 2\int_o^{\Pi} \int_o^{\eta} p \cos\theta \, Rd \, yd\theta \tag{38}$$

and

$$M = 2\int_o^{\Pi} \int_o^{\eta} p \cos\theta \, Ry \, dyd\theta \tag{39}$$

Numerical Computations

Numerical computations are performed for an axial-symmetric pier of configurations shown in Fig. 6. The pier is 100 feet in diameter with a cylindrical base 80 feet high and a conical top of 45 degrees extruding out of the water level which is 100 feet above the mud line. The incident wave is 7.6 seconds long in period and 14 feet high. The current velocity is null. This combination is chosen so that the numerical results can be compared with experiments of an identical situation (Wang, 1970).

To facilitate numerical computation, the pier is divided into

grids; 19 azimuthal stations from o to π, 8 depth stations on the cylindrical sections and 25 depth stations on the conical section (Fig. 6). The oncoming potential is calculated first according to Eq. (30) using a method similar to that developed by Wang and Hwang (1970).

The outflow potential is calculated by cutting short Eq. (34) to retain only the first two terms, i.e.,

$$\phi_{out}(\text{pile}) = \alpha_o \, \phi_{in}(\text{pile}) + \alpha_1 \frac{\partial \phi_{in}(p)}{\partial n} \tag{40}$$

The coefficients α_o and α_1 are obtained through iterative processes so that both boundary conditions, Eqs. (35) and (36) are approximately satisfied. In essence, the iterative scheme consists of the following manipulations:

1. Select a value of α_o (1 is selected for the present calculation because it leads to the case of cylindrical diffraction) and maintain C_1 to be zero. From Eq. (32), cutting short at two terms,

$$\phi = \sum_{k=0}^{1} \frac{\eta^k}{k!} \left[\frac{\partial^k \phi_{in}(p)}{\partial n^k} + \frac{\partial^k \phi_{out}(p)}{\partial n^k} \right]$$

and Eq. (30), we obtain a tentative velocity potential.

2. From Eq. (35), letting Γ_1 be equal to zero (exact solution) i.e.,

$$\frac{p}{\rho} = - \, g\eta + \phi_t + U\phi x - \frac{1}{2}(\nabla\phi)^2 = 0$$

a value of η can be obtained. Numerically, it is achieved by computing p at consecutive depth stations from the sea floor until p changes sign. If, for instance, the change of sign occurs between y_L and y_{L+1}, one calculates

$$\alpha = \frac{p_L}{p_L + p_{L+1}}$$

where p_L is the value of p at y_L and p_{L+1} that at y_{L+1}. The value of η is then determined as

$$\eta = y_L + \alpha \Delta y_L$$

If no change of sign occurs within reasonable range, the value of C_o needs to be adjusted.

3. If the value of η falls within a reasonable range, Eq. (36),

$$\frac{dp}{dt} < \Gamma_2$$

is used to check the validity of the solution. For the case $\frac{dp}{dt} > \Gamma_2$, letting $\Gamma_2 = 0$, we solve for α_1.

4. The above procedures are repeated until suitable sets of values of α_o and α_1 are obtained for all the azimuthal stations for a designated time station.

We have to confess that up to date no systematic method has been developed for the proper selection of α's. In the computer program, we have made the assumption that α_o varies from 1 (reflection from cylindrical surface) to 0 (the object has no influence on the wave field), and , varies from -1 to +1. Indeed, the results to date fall into this range. It is also impossible, at present, to establish the uniqueness of these solutions. At this moment, like many engineering problems, we rely on the actual physical situation to test the validity of our solution.

After we have obtained the velocity potential, the numerical computation of pressure distribution, forces and moments are rather straightforward. Only horizontal force and horizontal moments are being calculated.

Comparision of Theoretical and Experimental Results

Numerical computations are performed for the following input conditions:

pier diameter: 100 feet
water depth: 100 feet
wave height: 14 feet
wave period: 7.6 second
current velocity: 0 knots

These conditions are chosen so that the results can be compared with that obtained from earlier wave tank measurements. The experiments are described by Wang (1970). The essential results are summerized in Table 1. In this table, theoretical results based on linear wave theory and fifth-order wave theory are also included.

	Experiment	Cnoidal Wave	Fifth-Order Wave	Linear Wave
Wave Force (kips)	6,300	5,050	2,900	4,000 (est.)
Force Center (ft.)	53 (ave.)	49.5	49	

Table 1. Comparison of Experimental and Theoretical Results

From these results, it is clear that the results based on the modified cnoidal wave theory come closest to the experimental value. All three theories, however, yield smaller values than the experiment.

The total maximum horizontal force exerted on the pier is predicted by the cnoidal analysis to be approximately 20 percent smaller than the experiment, whereas the discrepancies become 30 percent and 45 percent for the cases of linear and fifth order wave methods, respectively. To explain why theories predict lower values than the experiments, several possibilities are examined.

All the theories are based on the assumption that the fluid is inviscid. As a consequence, viscous force, or velocity related force, is completely ignored in the computation. This assumption may or may not be valid, particularly in a scaled down model. If the viscous force cannot be ignored, the theoretical results would naturally be expected to yield smaller values than the experiments. In the report of experimental results, this possibility has been examined and discounted; because in the experiment, the observed wake is very small and the maximum horizontal force occurs at the instant when the water particle acceleration is maximum and its velocity is null at the center of the pier. This conclusion is further confirmed through comparing the theoretical pressure distribution with that of the experiment (Fig. 7). It is obvious from Fig. 7 that the effects of wake (from 150° to 180°) to the horizontal force is very small. The discrepancy actually occurs at the middle section of the pier.

A second possibility why the theoretically predicted force is smaller than the experiment is that the tank test was performed in a channel of finite width with channel width to pier diameter ratio equal to 4 to 1 whereas the theories deal with an infinite flow field. Thus, the blocking effect which might be expected to occur in the tank test has not been taken into consideration in the theoretical formulation. This blocking effect is believed to be the major contributing factor to the discrepancy between theoretical and experimental results.

Yet there exists a third possibility; namely, the selected wave theory does not truly represent the actual wave motion in the tank. This difficulty is rather insurmountable at this time. One can only hope that the selected wave theory is one of the better fits to the physical situation to be described. LeMéhante and Divoky (1968) have shown that among various wave theories, the cnoidal wave of MacCamy and Fuch comes closest to describing the water particle motions (rather than water surface variations which sometimes can be forced to fit) in shallow water. The present study seems to confirm, at least that among linear, fifth order and cnoidal, the cnoidal wave is a better choice. It is worthwhile to observe that under the combinations of shallow water and large obstacles, fifth order wave theory yields the largest discrepancy between theory and experiment. One may speculate that when the diameter of the object is of the same order of magnitude as the wave length, effects due to higher harmonics may nullify each other or may even interfere with that created by the basic harmonics.

Finally, in Fig. 8 the wet line on the cone-shaped surface of the pier is shown in comparison with the undisturbed wave shape (the wet line which occurs under the condition that the obstacle has no effect on the wave field) and with a fully reflected line (linear wave fully

reflected by a cylindrical structure). From the Figure, it is obvious that a cone-cylinder shaped structure causes far less surface disturbance than that caused by a cylindrical structure. As a consequence, a cone shaped structure also offers significant advantages over cylindrical structures in reducing wave forces. These phenomena concur the experimental results cited previously.

In summary, the mathematical model and the computer program developed provide a means of calculating wave forces and moments on large structures of irregular shapes in a wave field where the current effect cannot be neglected. The mathematical model, however, yields smaller wave forces than those obtained through experiment. It is believed to be suitable for engineering purposes provided that the characteristic length of the object is at least the same order of magnitude as the wave length and that the object is situated in a shallow-water wave environment. It is further stressed that this model will not yield validate information when the object is small compared to water depth and wave dimensions such as pilings and drill strings.

It is worth mentioning that in the derivation of inflow wave field, certain resilient figures of non-linear interference between current and shallow water waves have been discovered; those include wave length and wave height dispersions. Explicit expressions have been provided for these dispersions. Further pursuit in this direction should yield enlightening information in wave mechanics.

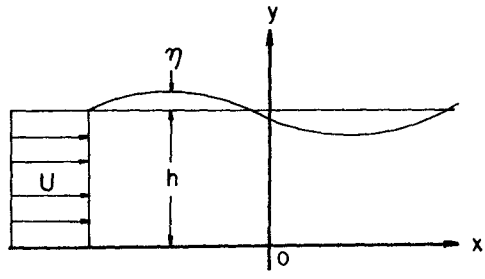

Figure 1. Definition sketch

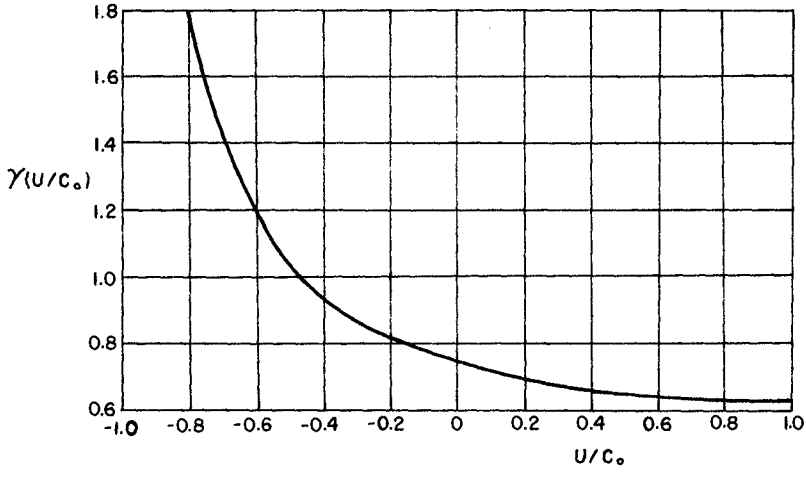

Figure 2. Variation of $\gamma(U/C_o)$ versus U/C_o

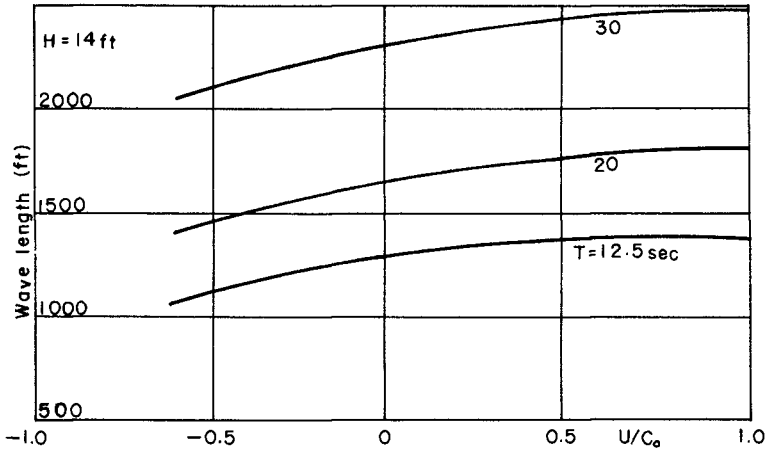

Figure 3. Current effect on wave length

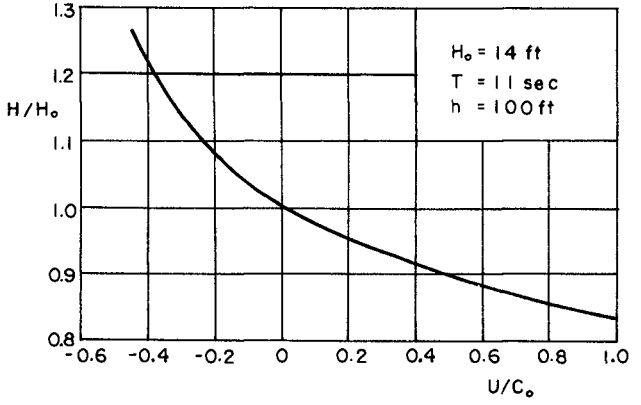

Figure 4. Current effect on wave height

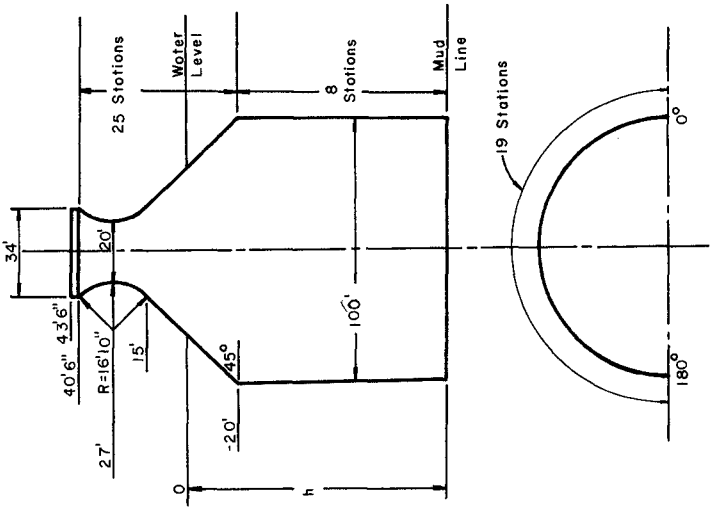

Figure 6. Grid system applied to obstacle for numerical computation

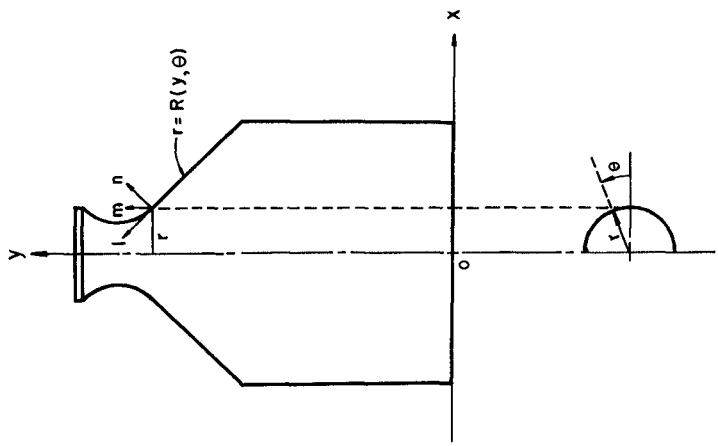

Figure 5. Definition and coordinate systems of obstacle

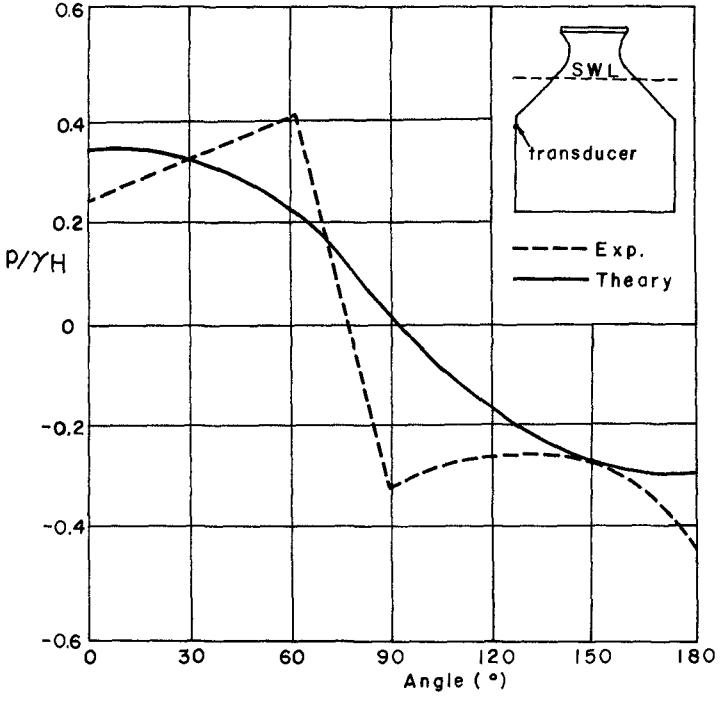

Figure 7. Pressure distributions about the obstacle at F_{max}

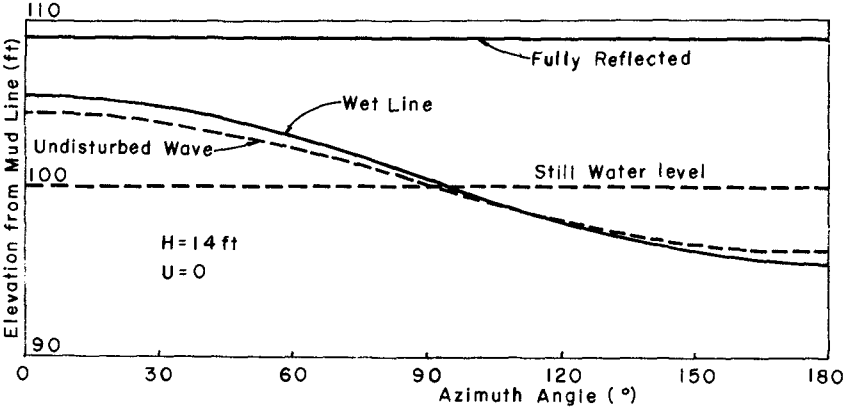

Figure 8. Wetline around the obstacle

References

1. Clavier, P. A., "Wave Effects on Piles of Any Symmetry in the Presence of Current," Supplement SN-425, National Engineering Science Co., 1967.

2. Le Méhauté, B., et.al., "Shallow Water Waves: A Comparison of Theory and Experiments," Proc. 11th International Conference on Coastal Engineering, 1968, pp. 86-107.

3. Longuet-Higgins, M. S. and Stewart, R. W., "Changes in the Force of Shut Gravity Waves on Long Waves and Tidal Current," Journal of Fluid Mechanics, 1960, pp. 565-583.

4. Keulegan, C. H. and G. W. Patterson, "Mathematical Theory of Irrotational Translation Waves," National Bureau of Standards, Paper RP1272, 1940.

5. MacCamy, R. C. and Fuch, R. A., "Wave Force on Piles; A Diffraction Theory," U. S. Army Corps of Engineers, Beach Erosion Board, T. M. No. 69, 1954.

6. Wang, H., "Loadings on Large Piers in Waves and Currents," Proc. 12th International Coastal Engineering Conference, pp. 1491-1511, 1970.

7. Wang, H. and Hwang, L. S., "Behavior of a Slender Body in Shallow-Water Waves," Proc. 12th International Coastal Engineering Conference, pp. 1723-1744, 1970.